LWT - Food Science and Technology 193 (2024) 115776

Contents lists available at ScienceDirect

LWT

journal homepage: www.elsevier.com/locate/lwt

A novel low-temperature procedure for oleogelation of heat-sensitive oils: Oleogels based on tucumã oil and ethyl cellulose

Priscila Dayane de Freitas Santos [a,b], Shaghayegh Keshanidokht [b], Saket Kumar [b], Mathias Porsmose Clausen [c], Matias Alejandro Via [c], Carmen Sílvia Favaro-Trindade [a], Mogens Larsen Andersen [b], Jens Risbo [b,*]

[a] College of Animal Science and Food Engineering, University of São Paulo, Avenida Duque de Caxias Norte, 225, 13635-900, Pirassununga, SP, Brazil
[b] Department of Food Science, University of Copenhagen, Rolighedsvej 26, DK-1958, Denmark
[c] Department of Green Technology, University of Southern Denmark, Campusvej 55, 5230, Odense M, Denmark

ARTICLE INFO

Keywords:
Carotenoids
Rheology
Tocopherols
Electron spin resonance
Microstructure

ABSTRACT

Oleogels are made by structuring oils with an oleogelator, e.g., ethyl cellulose (EC), and can be used as fat replacers in foods. Also, oleogels made from oils rich in bioactives, e.g., tucumã oil (TCO), could possess additional nutritional benefits. However, sensitive compounds are often degraded during the harsh conditions of most oleogelation procedures. Here we present an adapted low-temperature indirect method (IM) to structure TCO with EC, which is based on emulsification with aqueous ethanol as continuous phase, and the physicochemical properties are compared to oleogels with the same composition but produced by a direct method (DM) at high temperature. For IM, TCO was emulsified with EC ethanolic dispersions, followed by solvent removal and shearing. DM resulted in weak gels (G' < 10000 Pa), with low oil binding capacity (OBC) (12.63–66.26%), low carotenoid retention (CR) (20.7–31.6%) and complete depletion of α-tocopherol. Conversely, IM provided strong oleogels (G' > 10000 Pa), with high OBC (87.82–100.04%), CR (>95%) and α-tocopherol content (293–322 mg/kg). TCO oleogels with different physical properties and retention of sensitive compounds were obtained by DM and IM, showing the potential of IM oleogelation to preserve bioactives in the oleogels and producing healthier fat alternatives for the food industry.

1. Introduction

Oleogelation is a promising technique for the production of new food structures termed oleogels. These are solid-like materials obtained by structuring liquid lipids, usually vegetable oils, using so called oleogelators. The main advantage of edible oleogels is the possibility of partial or total substitution of solid saturated fats, thus improving the fatty acid profile of foods, without significantly affecting its textural properties (Martins et al., 2018).

The principle behind oleogelation is the formation of a three-dimensional network that entraps the oil, changing its physical properties from liquid to a firm gel-like structure (Li et al., 2022). This can be achieved by direct oleogelation, which consists of simply applying a heating step to dissolve the oleogelator in the oil phase, followed by a cooling step during which the structuring matrix is formed, and the oil mixture solidifies into a gel. One limitation of this technique is the low availability of food-grade materials with direct gelling ability that can be used as oleogelators. In fact, ethyl cellulose (EC, a semi-crystalline cellulose derivative) is one of the few food-grade polymers, if not the only one, capable of gelling oil directly (O'Sullivan et al., 2016; Pinto et al., 2021). Heating above its glass transition (~140 °C) or melting temperature (~180 °C) is necessary to dissolve it in the lipid phases. Subsequent cooling promotes interactions between EC chains through hydrogen bonding, resulting in a polymeric network (Davidovich-Pinhas et al., 2014; Davidovich-Pinhas, Gravelle, et al., 2015). The use of high temperatures in this process is a disadvantage since it accelerates oxidative degradation of many components of the lipid phase, especially polyunsaturated fatty acids, and bioactive compounds (Alongi et al., 2022; Zhang et al., 2019).

Conversely, indirect oleogelation approaches usually do not involve

* Corresponding author.
E-mail addresses: priscilafreitas@usp.br (P.D.F. Santos), shaghayegh@food.ku.dk (S. Keshanidokht), saket.kumar@food.ku.dk (S. Kumar), mpc@igt.sdu.dk (M.P. Clausen), mavia@igt.sdu.dk (M.A. Via), carmenft@usp.br (C.S. Favaro-Trindade), mola@food.ku.dk (M.L. Andersen), jri@food.ku.dk (J. Risbo).

https://doi.org/10.1016/j.lwt.2024.115776
Received 20 April 2023; Received in revised form 11 January 2024; Accepted 18 January 2024
Available online 20 January 2024

heating. Among them, the emulsion-templated method is based on preparation of an oil-in-water emulsion, followed by complete removal of the continuous phase through a drying process and shearing of the dried material (Patel et al., 2015). As a result, the microstructure of the obtained oleogels consists of oil droplets packed inside a network formed from the original emulsion interface (Tavernier et al., 2017). Apart from the use of low temperatures, another advantage of this method is the higher number of food-grade polymers suitable as emulsifiers/oleogelators to produce edible oleogels (Pinto et al., 2021). Frequently, water-soluble, and amphiphilic proteins (Tavernier et al., 2017; Vélez-Erazo et al., 2020), or polysaccharides (Espert et al., 2022; Meng et al., 2018) are used for this purpose.

However, some biopolymers like zein and EC are poorly soluble in both aqueous and oily phases at room temperature. Besides being food-grade, these polymers are abundant, commercially available, biodegradable, biocompatible, and are obtained from renewable resources (Ahmadi et al., 2022; Kasaai, 2018). Considering these examples of promising biopolymers with restricted application for indirect oleogelation, strategies to overcome this limitation should be created. In this sense, the concept of oil in ethanol/water emulsions and the possibility of emulsion stabilization based on ethanol-soluble components was evaluated by Keshanidokht et al. (2022). The promising results obtained suggests that a similar approach could be applied to other ethanol-soluble polymers, such as EC, to produce oleogels by the emulsion-templated method and thus avoid the extensive heating step required when EC is used in the direct method. The application of the emulsion-templated process could not only affect the chemical stability of the oleogel in comparison to the direct oleogelation method, but also the physical and rheological properties of the oleogel since the formation of the structuring network by the two techniques is based on different principles and leads to distinct microstructures.

Regarding the lipid phase, the use of oils containing bioactive compounds to produce oleogels would not only allow a reduction of saturated fat in foods but also improve the nutritional value of such products. In this sense, the fruits of *Astrocaryum vulgare* Mart, a palm tree native to the Amazon rainforest, have a pulp rich in unsaturated lipids that is consumed *in natura* in the northern Brazilian states. An orange oil known as tucumã oil (TCO) is extracted from the fruits' pulp. The oil contains high amounts of carotenoids and tocopherols, and shows antioxidant, anti-inflammatory and antihyperglycemic activities. Despite these promising properties, the application of TCO in the food industry is limited due to its instability under harsh processing conditions, such as the high temperatures used during direct oleogelation (Baldissera et al., 2017; Bony et al., 2012; Machado et al., 2022). In fact, both carotenoids and tocopherols are easily degraded at high temperatures or by oxidation (Park et al., 2018; Rodriguez-Amaya, 2001, p. 64) and this calls for a gentle method for oil gelation that does not involve heating.

There are no examples in the literature of the production of TCO oleogels by any oleogelation method; in addition, emulsion-templated oleogelation using EC as emulsifier/oleogelator has not been reported and a direct comparison of the consequences of either applying direct or indirect oleogelation with the same oleogelator has until now never been evaluated as the two principles normally require oleogelators with different solubility properties. This work is based on the hypothesis that different oleogelation procedures can significantly affect the final structures and physicochemical properties of oleogels presenting the same composition in terms of oil and oleogelator. Here we present a low-temperature process based on the emulsion-templated oleogelation, using oil in ethanol/water emulsions stabilized by EC, to produce TCO oleogels. Their properties in terms of rheology, oil binding capacity and retention of heat and oxidation-susceptible bioactives have been compared with EC oleogels of the same composition but made by the direct method involving high temperatures. We aim to demonstrate that by tuning the system using a third solvent (ethanol) it is possible to expand the emulsion-templated method to the use of oleogelators otherwise insoluble in water and to avoid the detrimental heating step of direct oleogelation.

2. Material and methods

2.1. Materials

TCO extracted by cold pressing was provided by Amazon Oil Industry (Ananindeua, Brazil), according to which the fatty acid profile of the oil consists of 23–28% palmitic acid, 2–3% stearic acid, 60–68% oleic acid, 1–2% vaccenic acid, 1–3% linoleic acid, and 2–4% linolenic acid. Ethyl cellulose, EC (viscosity of 10 cP; 9–11 mPa s; 5% in toluene/ethanol 80:20 (v/v); 48.0–49.5% ethoxy) was purchased from TCI Chemicals (Tokyo Chemical Industry Co., Tokyo, Japan). Hexane (95% n-Hexane, J.T.Baker®, Deventer, The Netherlands), ethanol (96%, Univar Solutions, Malmö, Sweden), ethyl acetate (CHROMASOLV®, for HPLC, ≥99.7%, Sigma-Aldrich, St. Louis, USA), n-heptane (CHEMSOLUTE®, for HPLC, min. 99.2%, Th. Geyer, Renningen, Germany) and PBN (N-*tert*-butyl-alpha-phenylnitrone, 98%, Alfa Aesar, Thermo Fisher Scientific, Haverhill, USA) were used to characterize the samples.

2.2. Production of tucumã oil oleogels

2.2.1. Direct method (DM)

TCO and EC oleogels were produced according to the direct method described by Zhang et al. (2019) with adaptations. EC (2.9, 5.7 and 8.2 g/100 g) and TCO were mixed and heated at 145 °C for 30 min using a hot plate with continuous magnetic stirring (~550 rpm), to promote dissolution of the polymer. Then, samples were cooled at room temperature (~25 °C) and allowed to set for at least 16 h before analysis. Pure TCO was also subjected to the heating conditions described above, and it was used as a control treatment sample. The oleogels were produced in triplicate.

2.2.2. Indirect method (IM)

An emulsion-templated oleogelation approach was adapted from Patel et al. (2015) and Keshanidokht et al. (2022) to prepare TCO and EC oleogels by emulsification at low temperatures. This process will be referred to as indirect method (IM). Initially, a preliminary study was carried out to evaluate the effects of oil loading (40–60 g/100 g), ethanol proportion in the solvent (70:30–90:10, v/v) and concentration of EC in ethanol solution (2–9 g/100 g) on the characteristics of the obtained oleogels. Based on these results (data not shown), oil loading and ethanol proportion were fixed at 50 g/100 g and 80:20 (v/v), respectively, and concentrations of EC in ethanol solution of 3, 6 and 9 g/100g were chosen. This gave IM oleogels with final EC concentrations of 2.9, 5.7 and 8.2 g/100 g (after evaporation of ethanol and water). Similar polymer proportions were used for production of TCO oleogels by DM.

In the first step of IM, ethanol:water (80:20, v/v) dispersions containing EC at 3, 6 and 9 g/100 g were made by stirring (Fisherbrand™ 3D Platform Rotator, Fisher Scientific, Waltham, USA) at 80 rpm for 36 h. Next, TCO and the dispersions (1:1, w/w, i.e., oil loading of 50 g/100 g) were emulsified at 12600 rpm for 4 min (ULTRA TURRAX IKA T25 digital, IKA®-Werke GmbH & CO., Staufen, Germany). Emulsions were dried at room temperature (~25 °C) for 46 h, to allow complete ethanol evaporation. Then, the samples were frozen at −80 °C (Sanyo Ultra Low, Buch & Holm, Copenhagen, Denmark) and freeze-dried for 24 h (Edwards, Buch % Holm, Copenhagen, Denmark). Finally, dry materials were manually sheared, resulting in TCO oleogels with final EC concentrations of 2.9, 5.7 and 8.2 g/100 g. During both oleogelation processes, the samples were protected from light to avoid degradation of the bioactive compounds in TCO. The oleogels were prepared in triplicate.

2.3. Physical characterization of tucumã oil oleogels

2.3.1. Rheology

Rheological properties of the oleogels were evaluated using a Discovery rheometer (Discovery HR-2 Hybrid Rheometer, TA Instruments, New Castle, USA) with a temperature control system. All experiments were carried out in triplicate (one measurement for three replicated experimental units of each treatment), using a 25 mm parallel plate geometry with crosshatched surface, and working gap of 1 mm. Data were analyzed using the software TRIOS (Version 5.1.1, TA Instruments, New Castle, USA).

2.3.1.1. Amplitude and frequency sweeps. The storage (G') and loss modulus (G'') of the samples were recorded over the range of oscillatory strain (γ) 0.01–1000% at a fixed angular frequency (ω) of 6.28 rad s^{-1} to determine the Linear Viscoelastic Region (LVR) and the crossover point ($G' = G''$). Then, angular frequencies varying from 100.0 to 0.1 rad s^{-1}, at a fixed strain of 0.05% (within the LVR), were used to evaluate the G' and G'' of oleogels over the applied ω. All the measurements were performed at 25 °C.

2.3.1.2. Temperature sweep. The thermal properties of oleogels, as expressed by G' and G'', were characterized over two temperature cycles, consisting of an initial heating from 25 to 150 °C, followed by cooling from 150 to 25 °C. This range was chosen based on the temperature applied for production of oleogels by DM. Experiments were conducted at fixed ω (6.28 rad.s-1) and γ (0.05%), with a heating/cooling rate of 5 °C.min^{-1}.

2.3.2. Oil binding capacity (OBC)

The OBC of oleogels was determined by centrifugation, according to Liu et al. (2020). About 1 g of each oleogel was added to previously weighed Eppendorf tubes, which were then centrifuged (Fisherbrand™ accuSpin™ Micro 17, Thermo Fisher Scientific, Osterode am Harz, Germany) at 10000×*g* for 10 min, at 25 °C. Next, the top layer consisting of released oil was removed, and the tubes were weighed again. The OBC, in %, was determined through Equation (1):

$$OBC\ (\%) = \frac{w_i}{w_f\ x\ \varphi}\ x\ 100 \qquad \text{Equation (1)}$$

where w_i and w_f are the initial and final weights of oleogel, respectively, in g; and φ is the proportion of oil composing the sample. Analyses were performed six times (two measurements for three replicated experimental units of each treatment).

2.3.3. Multi-photon microscopy

The oleogel microstructure was visualized by a combination of label-free multi-photon microscopy methods: coherent anti-Stokes Raman scattering (CARS) microscopy was used for visualizing the oil phase exciting the symmetric $–CH_2$ stretch (2845 cm^{-1}), while second harmonic generation (SHG)/multi-photon auto-fluorescence microscopy was used for simultaneous visualization of the EC phase. Imaging was done on a Leica SP8 microscope (Leica Microsystems GmbH, Mannhein, Germany) equipped with a picoEmerald multi-photon laser (APE, Berlin, Germany) operated at 1064 nm and 817 nm. The signal was recorded in the epi-direction splitting the CARS/SHG signals by a dichroic mirror at 560 nm and passing the signals through, respectively, a broadband 510/100 and a bandgap 661/11 Brightline HC filter (AHF analysentechnik AG, Tübingen, Germany) before detection on photomultiplier tube (PMT) detectors. All images were acquired at room temperature using a 40x HC PL IRAPO 1.1 NA Leica objective and adjusting the laser intensity for each sample. Samples were placed on #1.5 coverslips and images of 388 × 388 μm^2 and 150 nm pixel size were acquired at z = 10 μm distance from the glass surface. Imaging was done in triplicates on two independently prepared oleogel samples. For display, representative images were selected, a Gaussian blur background subtraction was performed, and images were contrast-enhanced to highlight structural features.

2.4. Chemical characterization of tucumã oil oleogels

2.4.1. Total carotenoid content

Total carotenoids of the oleogels and pure TCO (heated and unheated) were quantified according to O'Sullivan et al. (2017) with adaptations. For pure oil, about 0.01–0.03 g of sample was dissolved in 5 mL of hexane, and the absorbance of the solution was measured at 450 nm in a spectrophotometer (Evolution™ 350 UV–Vis Spectrophotometer, Thermo Scientific, Waltham, USA) using a quartz cuvette and hexane as blank. For oleogels, approximately 0.01–0.04 g of each material was added with 5 mL of hexane, and the mixtures were vortexed at 2200 rpm for 1 min (MS2 Minishaker, IKA, Wilmington, USA). Then, 1.5 mL of the liquid was transferred to an Eppendorf tube and centrifuged (Fisherbrand™ accuSpin™ Micro 17, Thermo Fisher Scientific, Osterode am Harz, Germany) at 17000×*g* for 15 min, at 25 °C. The absorbance of the supernatant was evaluated in the UV-VIS spectrophotometer under the same conditions. Analyses were carried out in quadruplicate (two measurements for two replicated experimental units of each treatment). And the total carotenoid content, in mg/kg_{sample}, was calculated from Equation (2) (Rodriguez-Amaya & Kimura, 2004):

$$Total\ carotenoid\ content\ (\mathrm{mg}/\mathrm{kg}) = (A\ x\ V\ x\ 10000) \,/\, \left(A^{1\%}_{1cm}\ x\ m\ x\ \varphi\right) \qquad \text{Equation (2)}$$

where A = absorbance, V = hexane volume (mL), $A^{1\%}_{1cm}$ = β-carotene absorption coefficient in hexane (2560, according to Hart and Scott (1995)); m = mass of sample (g); and φ is the oil fraction in the sample.

Carotenoid retention (expressed as %) in pure heated oil and oleogels was determined by comparing the total carotenoid contents of the samples to that of pure unheated oil.

2.4.2. α-Tocopherol content

The content of α-tocopherol in TCO oleogels was quantified by High Performance Liquid Chromatography (HPLC), using a Supelcosil LC-NH2 column (25 cm × 4.6 mm, 5 μm; Supelco, Sigma-Aldrich, St. Louis, USA), and coupled with a fluorescence detector (1260/1290 Infinity, Agilent Technologies, Santa Clara, USA). For α-tocopherol extraction, about 0.02–0.10 g of sample was dissolved in 1 mL of heptane and vortexed at 1800 rpm for 30 s (MS2 Minishaker, IKA, Wilmington, USA). The solutions were centrifuged (Fisherbrand™ accuSpin™ Micro 17, Thermo Fisher Scientific, Osterode am Harz, Germany) at 10000×*g* for 10 min (25 °C) and filtered (0.22 μm pore size). Isocratic elution was performed with heptane/ethyl acetate (70:30, v/v) as mobile phase, at 1 mL/min, for 14 min. The bioactive was detected at excitation and emission wavelengths of 295 and 330 nm, respectively, and quantified through an α-tocopherol calibration curve. Analyses were repeated six times (two measurements for three replicated experimental units of each treatment).

2.4.3. Oxidative stability evaluation by electron spin resonance (ESR)

The susceptibility to oxidation of pure TCO and TCO oleogels was assessed with ESR spectrometry (MiniScope MS 5000, Magnettech, Freiberg Instruments, Freiberg, Germany), using PBN as spin trap. Before analysis, the samples were mixed with a PBN solution in ethyl acetate (10.65 g/L) at 1:1 (w/v), and the mixtures were vortexed at 1800 rpm for 30 s (MS2 Minishaker, IKA, Wilmington, USA). Then, samples were stored under accelerated oxidation conditions, protected from light in a water bath at 60 °C (Julabo, Buch & Holm, Seelbach, Germany), for 24 h. At times 0, 4, 6, 8, 10, 12 and 24 h, an aliquot of each solution was taken with a 50 μL microcapillary tube and analyzed using magnetic field ranging from 325 to 350 mT, modulation amplitude of 0.2 mT and sweep time of 60 s. Determinations were performed in

quadruplicate (two measurements for two replicated experimental units of each treatment), at room temperature. Results were expressed as intensity of radical formation over time, which was determined by measuring the amplitude of the second peak of each spectrum (as indicated in Fig. S2).

2.5. Statistical analysis

Data were analyzed using Statistica software (STATISTICA, version 13.5.0.17, TIBCO Software Inc., Palo Alto, USA). ANOVA and post-hoc Tukey's tests were performed, with a significance level of 0.05.

3. Results

3.1. Preparation and physical characterization of tucumã oil oleogels

TCO was structured with EC through a direct method (DM) involving a heating step, and by an indirect method (IM) at low temperature, based on adaptation of the emulsion-templated approach, using oil in ethanol emulsions rather than oil in water emulsions in order to make EC soluble in the continuous phase. Oleogels produced by IM at all EC concentrations were solid-like, self-standing and with an intense orange color (Fig. 1). Apparently, increasing the proportion of EC had little impact on the visual characteristics of these materials. On the other hand, a clear effect of polymer concentration was observed for samples obtained by DM, since those with 2.9 and 5.7 g of EC/100 g appeared as viscous liquids, while a solid-like material was achieved only at 8.2 g of EC/100 g. In addition, DM oleogels had a clearly lighter orange color than the IM ones, which could indicate degradation of the natural carotenoids of the tucumã oil due to the heating involved in the process.

The rheological properties of the oleogels are presented in Figs. 2 and 3. According to the amplitude sweep rheograms (Fig. 2), at low strain (LVR) G' is higher than G'' for all samples, independent of the oleogelation method and EC concentration. Also, at 0.01% strain, IM samples show much higher G' and G'' values than DM samples (G' around 10^5–10^6 Pa for IM and 10^2–10^3 Pa for DM). For IM oleogels, the change in polymer proportion from 2.9 to 5.7 g/100 g caused an increase of approximately one order of magnitude in both rheological parameters (G' from ~10^5 to 10^6 Pa, and G'' from ~10^4 to 10^5 Pa), but no significant difference was observed after further increase of EC content. In contrast, G' and G'' increased with the amount of polymer added to DM formulations.

The LVR is quite similar for all oleogels, ranging from 0.01 to ~1% strain. The gradual decrease in both moduli above the LVR reveals that all samples presented shear thinning response upon deformation, resulting in eventual collapse of the polymer network and, ultimately, liquid flow ($G'' > G'$). Aguilar-Zárate et al. (2019) reported the same viscoelastic behavior for high oleic canola oil oleogels obtained with varying proportions of EC and lecithin by direct oleogelation. They observed that above the LVR (~1–5% strain), the G' and G'' of all samples decreased gradually, revealing elastic softening and viscous thinning due to the applied deformation.

Regarding the crossover point, where G' equals G'', a higher strain was necessary to change the behavior of IM samples (~300% strain), while values between 3 and 30% were enough to cause the same effect in DM oleogels. Briefly, this point indicates the yielding point or the transition of the material from a solid-like to a liquid-like behavior. The results suggest that IM produced structures with greater resistance upon deformation. In addition, for materials obtained by IM, the EC concentration did not affect the crossover strain, while for DM samples, the higher the amount of polymer, the higher the crossover strain. No comparable results were found in the literature for IM oleogels, but low crossover strains (~6%) have also been observed for high oleic safflower oil structured with EC (4 cP, 7% w/w) and glyceryl monostearate (GMS, 0.5–1.0% w/w) by direct oleogelation (García-Ortega et al., 2021).

Angular frequency sweep results (Fig. S1) revealed that rheological properties of the oleogels prepared by IM were not significantly affected over the studied range of frequency, while DM samples with the lowest EC proportions (2.9 and 5.7 g/100 g) showed frequency dependence, as revealed by a crossover between G' and G'' at values higher than 10 rad s^{-1}. This means that IM oleogels are more structured and stronger than frequency-dependent DM samples. Such an interpretation has also been presented by Khiabani et al. (2020), who observed that increasing the proportion of adipic acid in soybean oil-carnauba wax oleogels resulted in samples with less frequency dependence and, consequently, higher gel strength. Moreover, according to Li et al. (2017), materials with frequency independent storage and loss modulus are classified as "true gels", while those presenting frequency dependence are viscoelastic "pseudo-gels".

The influence of temperature on the rheological parameters of the

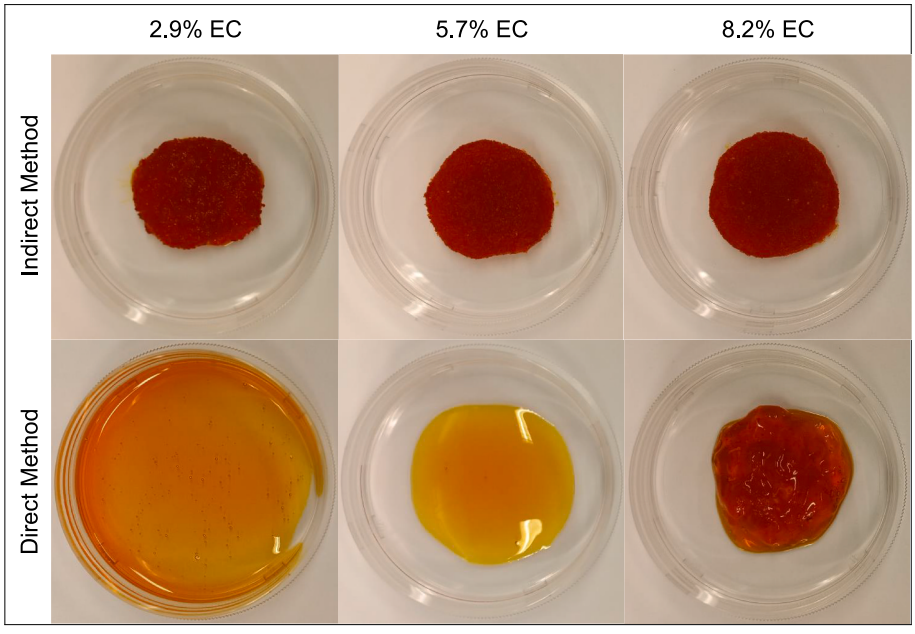

Fig. 1. TCO oleogels produced by direct (DM) and indirect (IM) methods at different EC concentrations (2.9, 5.7 and 8.2 g/100 g).

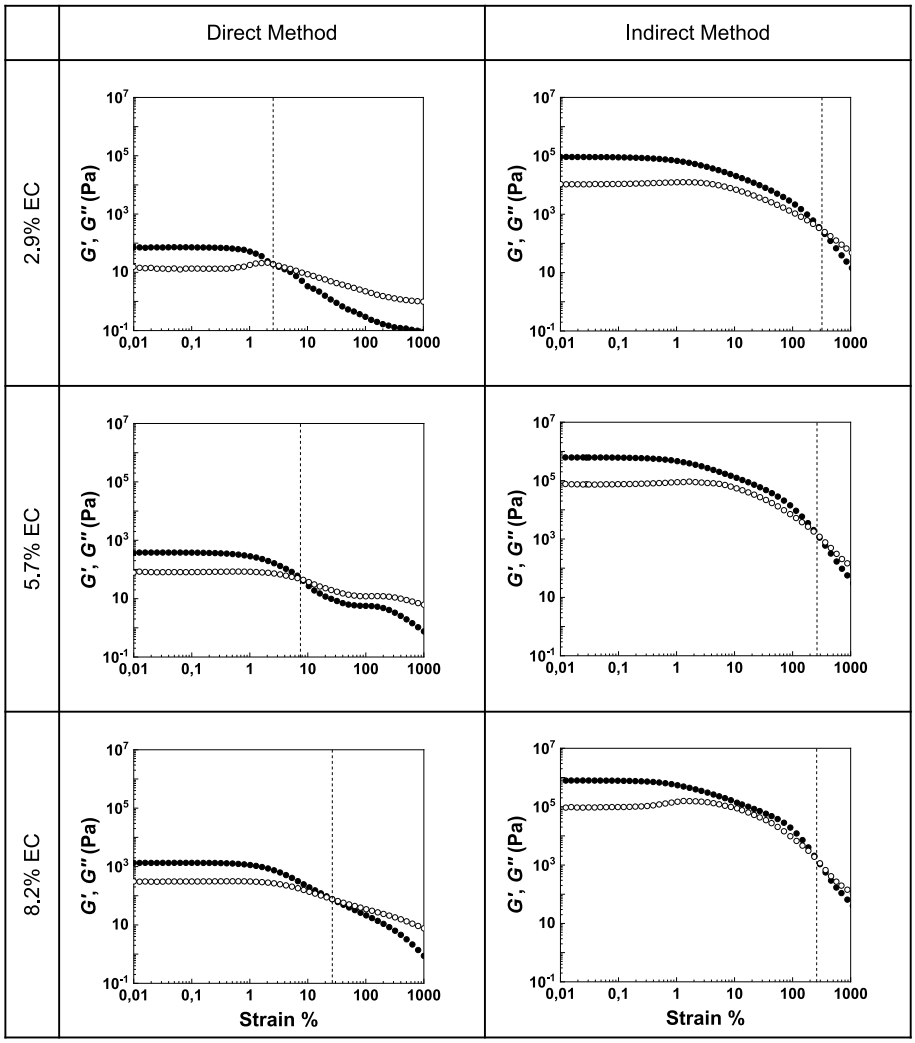

Fig. 2. Rheological properties of oleogels. Amplitude sweep curves of TCO oleogels obtained through DM and IM techniques (with 2.9, 5.7 and 8.2 g of EC/100 g) at 25 °C, over the oscillatory strain range of 0.01–1000% and a fixed angular frequency of 6.28 rad s^{-1}. In the graph: (●) G' and (◌) G''.

oleogels was also measured. The samples obtained by DM and IM show completely different behaviors after heating/cooling cycles (Fig. 3). G' and G'' of DM oleogels diminished progressively during heating from 25 to 150 °C, indicating that they become gradually softer as the temperature increases. Above approximately 100–120 °C, the storage and loss modulus could not be detected, as evidenced by the noisy curves, probably because of intense softening of the samples. However, it is not clear if the gels shift to liquid-like behavior at the end of heating since G' and G'' values cannot be effectively compared. Upon cooling, DM oleogels turn stronger and end up with higher G' and G'' than observed before heating. This difference between gel strength at the end of cooling and at the beginning of heating is less evident as the EC proportion changes from 2.9 to 8.2 g/100 g.

IM oleogels showed almost constant G' and G'' when heated up to ~110 °C, and a sharp decrease of the parameters happened above this temperature, revealing intense softening. Despite that, the behavior of samples did not become liquid-like since G' remained higher than G''. As the materials were cooled, the storage and loss modulus increased progressively until reaching a slight inflection point at about 70–80 °C, and below this temperature, stiffening was less pronounced. In this case, independent of EC concentration, oleogels were less strong after a heating/cooling cycle than before analysis.

IM oleogels presented higher oil binding capacity (OBC) (87.82–100.04%) than DM oleogels (12.63–66.26%) (Fig. 4). For samples made by direct oleogelation, the increase in EC concentration from 2.9 to 8.2 g/100 g resulted in significantly higher OBC values, revealing an almost linear dependency. A similar but less evident effect was found for IM oleogels. In this case, increasing EC proportion from 2.9 to 5.7 g/100 g improved the OBC of samples, but adding more polymer to the formulation had no significant impact on the OBC.

The microstructure of oleogels obtained by DM and IM at different EC proportions was evaluated by CARS (oil phase) and SHG microscopy (EC phase) (Fig. 5). Images show that the signals from the two phases are clearly separated from each other and complementary. The images further show DM samples were not as SHG active, giving a weaker signal, and that structures were more diffuse. On the other hand, the microstructure of IM oleogels can be seen as oil droplets of quite uniform size distribution, delimited by a thin EC network.

3.2. *Chemical characterization of tucumã oil oleogels*

Oleogels made by IM had high contents of total carotenoids, which did not significantly differ from the amount found in pure TCO (Table 1). In fact, the retention of carotenoids in these oleogels, calculated relative to the level of total carotenoids of unprocessed oil, was higher than 95% regardless of EC concentration. Heated TCO and DM oleogels, had much lower levels of total carotenoids compared to IM samples, and the carotenoid content decreased significantly from 31.6% to 20.7% as the

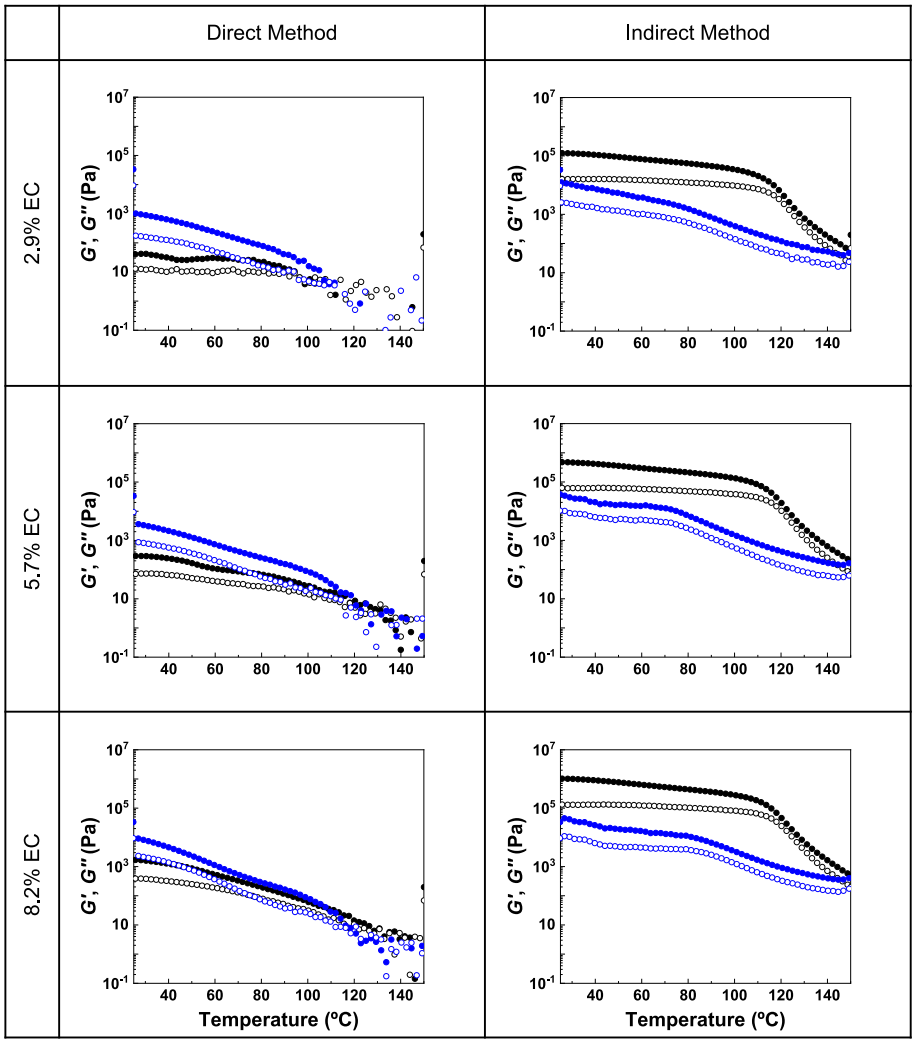

Fig. 3. Rheological properties of oleogels. Temperature sweep curves of TCO oleogels produced by DM and IM oleogelation, containing 2.9, 5.7 and 8.2 g of EC/100 g. A heating cycle from 25 to 150 °C was first performed, followed by a cooling cycle back to 25 °C. Measurements were carried out at fixed angular frequency (6.28 rad.s^{-1}) and strain (0.05%), with a heating/cooling rate of 5 °C.min^{-1}. In the graph: (●) *G'* – heating cycle; (○) *G''* – heating cycle; (◆) *G'* – cooling cycle; (◇) *G''* – cooling cycle.

proportion of EC increased from 2.9 to 8.2 g/100 g. Regarding α-tocopherol content, a slight decrease was seen as the amount of polymer was increased from 0 (pure oil) to 8.2 g/100 g, for oleogels produced indirectly, however, the decrease was found not to be statistically significant. Retention of this antioxidant in IM oleogels was above 89%. In contrast, α-tocopherol could not be detected in pure heated oil and DM oleogels most likely due to the harsher oxidative conditions during this preparation method.

The oxidative stability of the oleogels and pure TCO was evaluated by their tendency to generate radicals during gentle heating as evaluated by ESR spectroscopy. The ESR spectra of the different materials (Fig. S2) presented three broad lines with hyperfine coupling constant $a_N = 1.49$ mT, which is typical for nitroxyl spin adducts of lipid-derived radicals (Merkx et al., 2021; Velasco et al., 2005). The proton coupling constant (a_H) could not be determined due to line broadening. For all samples, radical formation occurs at a slow rate during the first 12 h of storage under accelerated oxidation conditions, but a sharp increase happens after this time (Fig. 6). Pure TCO and oleogels produced by IM gave higher levels of radicals, while the second group represents the pure heated oil and DM oleogels, which showed lower rates of radical formation.

4. Discussion

Indirect oleogelation was shown to be a gentle method for making oleogels without major losses of heat and oxidation sensitive components. Assessment of carotenoid retention in oleogels after gelation has not been previously reported, but some studies have evaluated the degradation of other bioactives during oleogelation. Alongi et al. (2022) observed losses of α-tocopherol, tyrosol and hydroxytyrosol of ~37, 53 and 52%, respectively after structuring extra virgin olive oil with EC, and they attributed these results to the high temperature used during the process (140 °C). In addition, the extent of degradation was dependent upon the type of oleogelator and its gelation temperature, since structuring the same oil with saturated monoglycerides caused less oxidation of bioactives (~31, 23 and 22%, for α-tocopherol, tyrosol and hydroxytyrosol, respectively) as the result of a milder heating process (80 °C).

In the present study, DM oleogels had a visually lighter orange color than IM gels, indicating that carotenoids were degraded due to the extensive heating involved in the DM oleogelation, and this loss was confirmed by the lower carotenoid content of DM samples. Besides oxidation, carotenoids undergo *cis-trans* isomerization when exposed to high temperatures, as recently modelled by Schjoerring-Thyssen et al. (2020). The almost complete retention of carotenoids in IM oleogels can

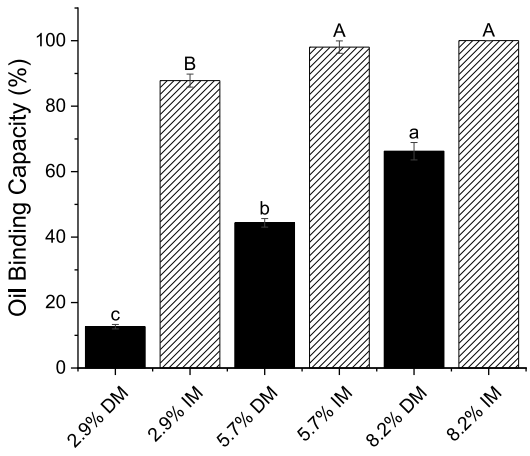

Fig. 4. Oil binding capacity (%) of oleogels produced by DM and IM methods, containing 2.9, 5.7 and 8.2 g of EC/100 g. Values are mean ± standard deviation (n = 6). Different lower case/capital letters indicate significant differences ($p < 0.05$) at varying EC proportions, for a fixed method.

thus be explained by the milder temperatures during their preparation. A small decrease in carotenoid retention was observed for DM samples with increased EC content. This is seemingly in contrast with the findings of Cui et al. (2019), who reported that increasing the proportion of structuring agent (monoglyceride) from 10 to 20 g/100 g improved β-carotene retention from 49.81 to 71.85%, in corn oil oleogels stored for 24 days at 25 °C. According to the authors, the higher content of structuring agent produced a more compact and stronger gel network, which acted as a physical barrier to prevent the mobility of β-carotene within the oleogel and the diffusion of oxidative species into the samples. This protective effect was not observed for the range of EC proportions evaluated in the present study.

α-Tocopherol was preferentially oxidized over carotenoids in TCO oleogels, as carotenoids could be quantified in DM samples, whereas the α-tocopherol content was below the detection limit. Oxidized carotenoids can be regenerated by α-tocopherol thus preserving the pigments (Shibasaki-Kitakawa et al., 2004; Yi et al., 2011). These results have an interesting relationship with those of ESR analysis. Pure heated oil and DM samples showed a lower intensity of radical formation than unheated TCO and IM oleogels, which had the highest carotenoid levels. According to Menezes et al. (2022), TCO contains approximately 65% oleic acid, 26% palmitic acid and a low level of polyunsaturated fatty acids (less than 10%). This makes the oil only moderately sensitive towards radical initiated autoxidation. It is therefore likely that the main oxidation and radical generating event occurring in TCO and the oleogels is the degradation of the more easily oxidized carotenoids and tocopherols, rather than the oxidation of unsaturated fatty acids. This is in agreement with results found by Shibasaki-Kitakawa et al. (2004) who studied the oxidation kinetics of β-carotene in oleic acid in the presence of α-tocopherol. Considering that carotenoids may act as antioxidants or prooxidants depending on medium characteristics and that β-carotene (the major carotenoid in TCO) has been demonstrated to have prooxidant effects (Ribeiro et al., 2018; Zeb & Murkovic, 2011, 2013), the high concentration of these pigments in the pure oil and IM oleogels might have accelerated their oxidation, leading to intense radical formation. This hypothesis corroborates with the findings of a study by Henry et al. (1998), in which the presence of β-carotene at low levels did not affect the oxidative stability of heated safflower oil, but where concentrations higher than 500 ppm resulted in pro-oxidant activity and faster lipid degradation (Henry et al., 1998).

The macroscopic appearance of TCO oleogels reveals that the oleogelation method had a major impact on the physical properties of the samples. In fact, IM resulted in solid-like, self-standing oleogels even at the lower EC concentration, which indicates that the dissolution and arrangement of EC molecules may be more important than polymer concentration on defining the oleogel structure.

The production of stiff polymeric gels relies on the formation of many interactions between polymer chains, which occur more easily when their dispersion in the oil/solvent is thermodynamically favorable (Gravelle et al., 2016). Considering the oleogelation processes used in this study, it is possible that the IM facilitated hydrogen bonding between EC molecules, since the polymer was completely dissolved in the ethanol solution before emulsification, and consequently that its chains were more extended and likely to interact with each other during gelation. This, in turn, would result in a higher level of structure formation, i.e., in a more organized and stronger microstructure. On the other hand, during DM, incomplete dissolution of EC possibly happened in the heating step, thus reducing the number of chains available for network formation after cooling, producing a weaker microstructure (Davidovich-Pinhas et al., 2014; Liu et al., 2020). Indeed, samples were heated just above the glass transition temperature of EC, not above its melting temperature, so the polymer was likely not fully dispersed in the oil/solvent. The information above may explain why DM oleogels were much softer and less resistant to deformation than the IM samples, despite their composition being the same.

Imaging of the oleogels by multi-photon microscopy also showed clear microstructural differences between samples obtained by DM and IM. The weak SHG signals in DM oleogels may be related to the formation of a weak and amorphous polymeric network, since this type of microscopy has been used before for evaluation of semi-crystalline and crystalline materials (Brüggemann et al., 2010; Song et al., 2018; Soto et al., 2017). In fact, fading of SHG signal was associated with loss of crystallinity during heating and swelling of starch in previous works (Brackmann et al., 2011; Nessi et al., 2018). The translucent aspect of DM oleogels obtained in the present study is further evidence of their amorphous character. The three-dimensional network assembled after direct gelation of EC-oleogels was previously elucidated as a coral-like polymer frame, with irregular pores of micrometric size which are filled with the oil phase (Zetzl et al., 2014). Conversely, the effective assessment of IM oleogels' microstructure by SHG suggests that polymer-polymer interactions were possibly favored during solvent removal, leading to a more dense and organized, semi-crystalline structure, which explains the improved rheological properties of these samples compared to DM ones. These results also make sense when considering the OBC of the samples, since IM oleogels showed little to no oil loss, due to their strong and highly structured polymeric network.

Regarding the thermal behavior of the oleogels, all samples were thermo-reversible, regardless of gelation method and EC concentration, meaning that they could restore their gel properties after thermal treatment. However, hysteresis between the rheological parameters obtained in the heating and cooling steps suggests only partial reversibility, as demonstrated by findings of previous works (Davidovich-Pinhas, Gravelle, et al., 2015; Principato et al., 2021). Increasing temperature caused continuous weakening of DM oleogels due to disruption of hydrogen bonds stabilizing the three-dimensional network. In the case of IM oleogels, slight changes in both moduli occurred during heating up to ~110 °C, indicating these samples were more thermostable than DM oleogels over this temperature range. It is possible that the higher level of organization of IM oleogels, as evidenced by the microscopy analysis, could have protected the gel structure from destabilization, even at high temperatures.

The different behavior of DM and IM oleogels at the end of the heating/cooling cycles may be understood considering the effects of EC dissolution and the cooling rate on gel strength. According to Davidovich-Pinhas, Gravelle, et al. (2015), the lower the cooling rate after gelation, the stronger the oleogels, because the polymer chains have enough time to arrange themselves in a more organized network, with more junction zones, resulting in higher strength. This hypothesis can

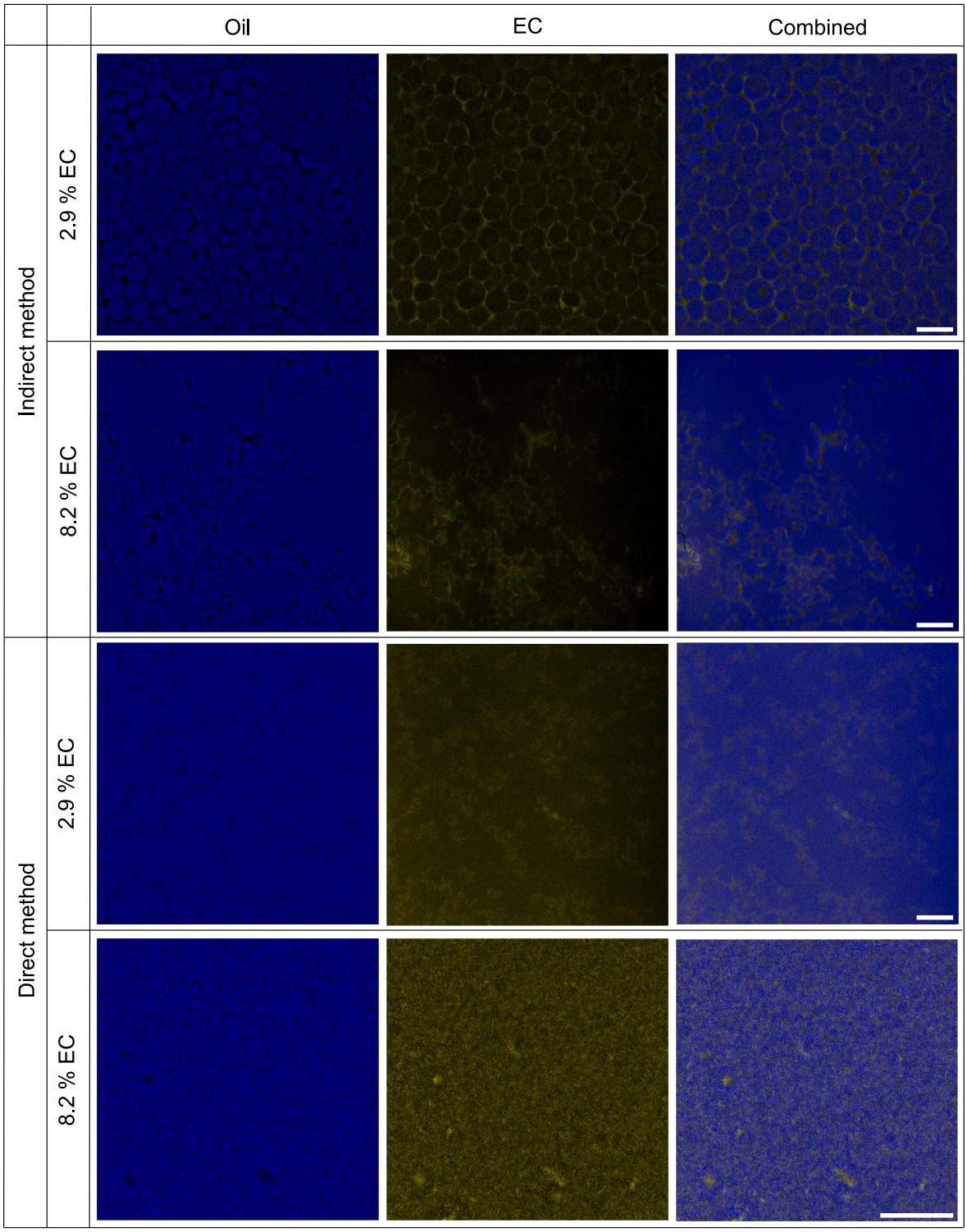

Fig. 5. Microscopy images of oleogels made with IM and DM using 2.9 and 8.2 g of EC/100 g. The oil-phase (blue) is visualized with CARS microscopy, while EC (yellow) is visualized using SHG microscopy. The overlays show the complementary signal of the two phases. Scale bars 50 μm (notice that the bottom panel has a longer scale bar). (For interpretation of the references to color in this figure legend, the reader is referred to the Web version of this article.)

explain the thermal behavior of DM oleogels, considering that the cooling rate was not controlled during oleogelation, and led to the formation of a weak structure, as confirmed by microscopy images. Conversely, a controlled and low cooling rate was applied during rheology experiments (5 °C·min^{-1}), allowing the EC molecules to form a stronger network. In the case of IM oleogels, their stiff and more organized structure was partially lost after the heating cycle, and, considering the absence of the ethanol solution that ensured complete EC dissolution during IM oleogelation, and the properties of the samples became similar to the DM oleogels. As a result, the restructuring of the gel network during cooling was limited by a lower number of junction zones between EC chains, leading to softer IM oleogels. However, these explanations are limited by the lack of analyses evidencing the potentially different number of interactions/bonds among EC molecules in the

Table 1
Contents of bioactive compounds of pure TCO and TCO oleogels obtained by direct and indirect oleogelation methods.

Sample	Total carotenoid content (mg/kg)	Carotenoid retention[a] (%)	α-tocopherol content (mg/kg)	α-tocopherol retention[b] (%)
Indirect method				
TCO	1129 ± 12^{a}	–	330 ± 28^{a}	–
2.9% IM	1123 ± 23^{a}	97.5 ± 2.0^{a}	322 ± 32^{ab}	98 ± 12^{a}
5.7% IM	1096 ± 26^{a}	95.2 ± 2.3^{a}	300 ± 6^{ab}	91 ± 7^{a}
8.2% IM	1105 ± 8^{a}	95.9 ± 0.7^{a}	293 ± 17^{b}	89 ± 9^{a}
Direct method				
HTCO	326 ± 39^{A}	28.3 ± 3.4^{A}	–	–
2.9% DM	364 ± 13^{A}	31.6 ± 1.1^{A}	–	–
5.7% DM	265 ± 9^{B}	23.0 ± 0.8^{B}	–	–
8.2% DM	239 ± 12^{B}	20.7 ± 1.0^{B}	–	–

Values are mean ± standard deviation (n = 4–6). Different lower case/capital letters in the same column indicate significant differences ($p < 0.05$) at varying EC10 proportions, for a fixed method. TCO: pure oil; HTCO: pure heated oil; IM: indirect method; DM: direct method.

[a] In terms of the carotenoid content in the pure oil.

[b] In terms of the α-tocopherol content in the pure oil.

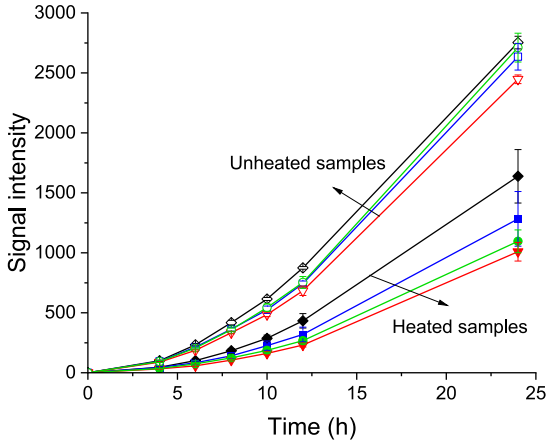

Fig. 6. Formation of PBN spin adducts detected by ESR spectroscopy due to oxidation of pure TCO and TCO oleogels produced by DM and IM, during storage at 60 °C in the dark. Signal intensity is reported as the amplitude of the second peak in the ESR spectra. Values are mean ± standard deviation (n = 4). In the graph: (—◇—) pure oil; (—◆—) pure heated oil; (—□—) 2.9% IM; (—■—) 2.9% DM; (—▽—) 5.7% IM; (—▼—) 5.7% DM; (—○—) 8.2% IM; (—●—) 8.2% DM.

DM and IM oleogels, which could confirm the correlation of the level of polymer arrangement and network organization with the strength of oleogels.

According to Patel et al. (2015), structured materials with a hardness in the range 0.4–3.0 N are defined as soft solids, while oleogels should present a gel stiffness $G' > 10000$ Pa. Using this definition, none of the samples produced by DM in the present work could be classified as oleogels, since their storage modulus ranged from 71 to 1325 Pa. Nevertheless, recent papers report the direct oleogelation of different oils using EC as oleogelator, and define the obtained materials as oleogels, despite most of them also showing $G' < 10000$ Pa (Eisa et al., 2020; Fu et al., 2020; Liu et al., 2020; Zhang et al., 2019). Herein, only the materials obtained by IM can be called oleogels based on their rheological properties (90786 Pa $< G' <$ 795403 Pa).

5. Conclusion

An adapted oil in ethanol emulsion-templated approach and direct oleogelation were successfully applied to structure TCO with EC, resulting in oleogels with completely different physical and chemical properties. The use of EC for indirect oleogelation, reported here for the first time, promoted high levels of structuring even at low polymer concentrations, which is interesting from industrial production perspective due to reduced cost and smaller percentage of non-oil components in the final product. In addition, the obtained samples may find many applications in the food industry, including in formulations processed under high shear and heating conditions, such as bakery products, processed meats, and cheeses. In fact, the functionality of IM oleogels would be retained after harsh food processes, considering their physicochemical and rheological properties. Moreover, the visual aspect of the oleogels, i.e., the orange color, could provide interesting sensory attributes to the cited products. Overall, it is concluded that TCO oleogels possess promising characteristics for replacement of saturated fat in foods in parallel to their enrichment with bioactive compounds, resulting in nutritionally improved products.

CRediT authorship contribution statement

Priscila Dayane de Freitas Santos: Writing – review & editing, Writing – original draft, Visualization, Validation, Project administration, Methodology, Investigation, Formal analysis, Conceptualization. **Shaghayegh Keshanidokht:** Writing – review & editing, Methodology, Investigation, Conceptualization. **Saket Kumar:** Writing – review & editing, Validation, Methodology, Investigation. **Mathias Porsmose Clausen:** Writing – review & editing, Investigation, Formal analysis. **Matias Alejandro Via:** Writing – review & editing, Investigation, Formal analysis. **Carmen Sílvia Favaro-Trindade:** Writing – review & editing, Supervision, Resources, Methodology, Funding acquisition, Conceptualization. **Mogens Larsen Andersen:** Writing – review & editing, Validation, Methodology, Conceptualization. **Jens Risbo:** Writing – review & editing, Validation, Supervision, Resources, Project administration, Methodology, Conceptualization.

Declaration of competing interest

The authors declare that they have no known competing financial interests or personal relationships that could have appeared to influence the work reported in this paper.

Data availability

Data will be made available on request.

7 Acknowledgements

The authors would like to thank the Coordenação de Aperfeiçoamento de Pessoal de Nível Superior (CAPES) for funding the mobility of P. D. F. Santos to the University of Copenhagen through the Program CAPES-PrInt (process number 88887.571710/2020–00). The work was supported by the Villum Foundation (Denmark) through a grant to M. P. C. (no. 00025414) and imaging was done using Danish Molecular Biomedical Imaging Center DaMBIC at SDU.

Appendix A. Supplementary data

Supplementary data to this article can be found online at https://doi.

org/10.1016/j.lwt.2024.115776.

References

Aguilar-Zárate, M., Macias-Rodriguez, B. A., Toro-Vazquez, J. F., & Marangoni, A. G. (2019). Engineering rheological properties of edible oleogels with ethylcellulose and lecithin. *Carbohydrate Polymers, 205*, 98–105. https://doi.org/10.1016/j.carbpol.2018.10.032

Ahmadi, P., Jahanban-Esfahlan, A., Ahmadi, A., Tabibiazar, M., & Mohammadifar, M. (2022). Development of ethyl cellulose-based formulations: A perspective on the novel technical methods. *Food Reviews International, 38*(4), 685–732. https://doi.org/10.1080/87559129.2020.1741007

Alongi, M., Lucci, P., Clodoveo, M. L., Schena, F. P., & Calligaris, S. (2022). Oleogelation of extra virgin olive oil by different oleogelators affects the physical properties and the stability of bioactive compounds. *Food Chemistry, 368*(August 2021), Article 130779. https://doi.org/10.1016/j.foodchem.2021.130779

Baldissera, M. D., Souza, C. F., Grando, T. H., Cossetin, L. F., Sagrillo, M. R., Nascimento, K., da Silva, A. S., Machado, A. K., da Cruz, I. B. M., Stefani, L. M., Klein, B., Wagner, R., & Monteiro, S. G. (2017). Antihyperglycemic, antioxidant activities of tucumã oil (*Astrocaryum vulgare*) in alloxan-induced diabetic mice, and identification of fatty acid profile by gas chromatograph: New natural source to treat hyperglycemia. *Chemico-Biological Interactions, 270*, 51–58. https://doi.org/10.1016/j.cbi.2017.04.001

Bony, E., Boudard, F., Brat, P., Dussossoy, E., Portet, K., Poucheret, P., Giaimis, J., & Michel, A. (2012). Awara (*Astrocaryum vulgare* M.) pulp oil: Chemical characterization, and anti-inflammatory properties in a mice model of endotoxic shock and a rat model of pulmonary inflammation. *Fitoterapia, 83*, 33–43. https://doi.org/10.1016/j.fitote.2011.09.007

Brackmann, C., Bengtsson, A., Alminger, M. L., Svanberg, U., & Enejder, A. (2011). Visualization of β-carotene and starch granules in plant cells using CARS and SHG microscopy. *Journal of Raman Spectroscopy, 42*(4), 586–592. https://doi.org/10.1002/jrs.2778

Brüggemann, D. A., Brewer, J., Risbo, J., & Bagatolli, L. (2010). Second harmonic generation microscopy: A tool for spatially and temporally resolved studies of heat induced structural changes in meat. *Food Biophysics, 5*(1), 1–8. https://doi.org/10.1007/s11483-009-9137-4

Cui, M., Mao, L., Lu, Y., Yuan, F., & Gao, Y. (2019). Effect of monoglyceride content on the solubility and chemical stability of β-carotene in organogels. *LWT - Food Science and Technology, 106*, 83–91. https://doi.org/10.1016/j.lwt.2019.02.042

Davidovich-Pinhas, M., Barbut, S., & Marangoni, A. G. (2014). Physical structure and thermal behavior of ethylcellulose. *Cellulose, 21*(5), 3243–3255. https://doi.org/10.1007/s10570-014-0377-1

Davidovich-Pinhas, M., Barbut, S., & Marangoni, A. G. (2015). The gelation of oil using ethyl cellulose. *Carbohydrate Polymers, 117*, 869–878. https://doi.org/10.1016/j.carbpol.2014.10.035

Davidovich-Pinhas, M., Gravelle, A. J., Barbut, S., & Marangoni, A. G. (2015). Temperature effects on the gelation of ethylcellulose oleogels. *Food Hydrocolloids, 46*, 76–83. https://doi.org/10.1016/j.foodhyd.2014.12.030

Eisa, A. H., Laufer, S., Rosen-Kligvasser, J., & Davidovich-Pinhas, M. (2020). Stabilization of ethyl-cellulose oleogel network using lauric acid. *European Journal of Lipid Science and Technology, 122*(2), 1–10. https://doi.org/10.1002/ejlt.201900044

Espert, M., Hernández, M. J., Sanz, T., & Salvador, A. (2022). Rheological properties of emulsion templated oleogels based on xanthan gum and different structuring agents. *Current Research in Food Science, 5*(March), 564–570. https://doi.org/10.1016/j.crfs.2022.03.001

Fu, H., Lo, Y. M., Yan, M., Li, P., & Cao, Y. (2020). Characterization of thermo-oxidative behavior of ethylcellulose oleogels. *Food Chemistry, 305*, Article 125470. https://doi.org/10.1016/j.foodchem.2019.125470

García-Ortega, M. L., Toro-Vazquez, J. F., & Ghosh, S. (2021). Development and characterization of structured water-in-oil emulsions with ethyl cellulose oleogels. *Food Research International, 150*(PB), Article 110763. https://doi.org/10.1016/j.foodres.2021.110763

Gravelle, A. J., Davidovich-Pinhas, M., Zetzl, A. K., Barbut, S., & Marangoni, A. G. (2016). Influence of solvent quality on the mechanical strength of ethylcellulose oleogels. *Carbohydrate Polymers, 135*, 169–179. https://doi.org/10.1016/j.carbpol.2015.08.050

Hart, D. J., & Scott, K. J. (1995). Development and evaluation of an HPLC method for the analysis of carotenoids in foods, and the measurement of the carotenoid content of vegetables and fruits commonly consumed in the UK. *Food Chemistry, 54*(1), 101–111. https://doi.org/10.1016/0308-8146(95)92669-B

Henry, L. K., Catignani, C. L., & Schwartz, S. J. (1998). The influence of carotenoids and tocopherols on the stability of safflower seed oil during heat-catalyzed oxidation. *JAOCS, Journal of the American Oil Chemists' Society, 75*(10), 1399–1402. https://doi.org/10.1007/s11746-998-0189-2

Kasaai, M. R. (2018). Zein and zein -based nano-materials for food and nutrition applications: A review. *Trends in Food Science and Technology, 79*(October 2017), 184–197. https://doi.org/10.1016/j.tifs.2018.07.015

Keshanidokht, S., Alejandro, M., Yucel, C., Porsmose, M., & Risbo, J. (2022). Zein-stabilized emulsions by ethanol addition ; stability and microstructure. *Food Hydrocolloids, 133*, Article 107973. https://doi.org/10.1016/j.foodhyd.2022.107973

Khiabani, A. A., Tabibiazar, M., Roufegarinejad, L., Hamishehkar, H., & Alizadeh, A. (2020). Preparation and characterization of carnauba wax/adipic acid oleogel : A new reinforced oleogel for application in cake and beef burger. *Food Chemistry, 333*, Article 127446. https://doi.org/10.1016/j.foodchem.2020.127446

Li, X., Saleh, A. S. M., Wang, P., Wang, Q., Yang, S., Zhu, M., Duan, Y., & Xiao, Z. (2017). Characterization of organogel prepared from rice bran oil with cinnamic acid. *Food Biophysics, 12*, 356–364. https://doi.org/10.1007/s11483-017-9491-6

Li, Y., Zou, Y., Que, F., & Zhang, H. (2022). Recent advances in fabrication of edible polymer oleogels for food applications. *Current Opinion in Food Science, 43*, 114–119. https://doi.org/10.1016/j.cofs.2021.11.007

Liu, N., Lu, Y., Zhang, Y., Gao, Y., & Mao, L. (2020). Surfactant addition to modify the structures of ethylcellulose oleogels for higher solubility and stability of curcumin. *International Journal of Biological Macromolecules, 165*, 2286–2294. https://doi.org/10.1016/j.ijbiomac.2020.10.115

Machado, A. P. F., Nascimento, R. P., Alves, M. R., Reguengo, L. M., & Marostica Junior, M. R. (2022). Brazilian tucumã-do-Amazonas (*Astrocaryum aculeatum*) and tucumã-do-Pará (*Astrocaryum vulgare*) fruits: Bioactive composition, health benefits, and technological potential. *Food Research International, 151*, Article 110902. https://doi.org/10.1016/j.foodres.2021.110902

Martins, A. J., Vicente, A. A., Cunha, R. L., & Cerqueira, M. A. (2018). Edible oleogels: An opportunity for fat replacement in foods. *Food & Function, 9*(2), 758–773. https://doi.org/10.1039/c7fo01641g

Menezes, E. G. O., Barbosa, J. R., Pires, F. C. S., Ferreira, M. C. R., de Souza e Silva, A. P., Siqueira, L. M. M., & de Carvalho Junior, R. N. (2022). Development of a new scale-up equation to obtain Tucumã-of-Pará (*Astrocaryum vulgare* Mart.) oil rich in carotenoids using supercritical CO_2 as solvent. *The Journal of Supercritical Fluids, 181*, Article 105481. https://doi.org/10.1016/j.supflu.2021.105481

Meng, Z., Qi, K., Guo, Y., Wang, Y., & Liu, Y. (2018). Macro-micro structure characterization and molecular properties of emulsion-templated polysaccharide oleogels. *Food Hydrocolloids, 77*, 17–29. https://doi.org/10.1016/j.foodhyd.2017.09.006

Merkx, D. W. H., Plankensteiner, L., Yu, Y., Wierenga, P. A., Hennebelle, M., & Van Duynhoven, J. P. M. (2021). Evaluation of PBN spin-trapped radicals as early markers of lipid oxidation in mayonnaise. *Food Chemistry, 334*, Article 127578. https://doi.org/10.1016/j.foodchem.2020.127578

Nessi, V., Rolland-Sabaté, A., Lourdin, D., Jamme, F., Chevigny, C., & Kansou, K. (2018). Multi-scale characterization of thermoplastic starch structure using Second Harmonic Generation imaging and NMR. *Carbohydrate Polymers, 194*, 80–88. https://doi.org/10.1016/j.carbpol.2018.04.030

O'Sullivan, C. M., Barbut, S., & Marangoni, A. G. (2016). Edible oleogels for the oral delivery of lipid soluble molecules: Composition and structural design considerations. In *Trends in food science and technology* (Vol. 57)Elsevier Ltd. https://doi.org/10.1016/j.tifs.2016.08.018.

O'Sullivan, C. M., Davidovich-Pinhas, M., Wright, A. J., Barbut, S., & Marangoni, A. G. (2017). Ethylcellulose oleogels for lipophilic bioactive delivery-effect of oleogelation on in vitro bioaccessibility and stability of beta-carotene. *Food & Function, 8*(4), 1438–1451. https://doi.org/10.1039/c6fo01805j

Park, C., Bemer, H. L., & Maleky, F. (2018). Oxidative stability of rice bran wax oleogels and an oleogel cream cheese product. *Journal of the American Oil Chemists Society, 95*(10), 1267–1275. https://doi.org/10.1002/aocs.12095

Patel, A. R., Rajarethinem, P. S., Cludts, N., Lewille, B., De Vos, W. H., Lesaffer, A., & Dewettinck, K. (2015). Biopolymer-based structuring of liquid oil into soft solids and oleogels using water-continuous emulsions as templates. *Langmuir, 31*(7), 2065–2073. https://doi.org/10.1021/la502829u

Pinto, T. C., Martins, A. J., Pastrana, L., Pereira, M. C., & Cerqueira, M. A. (2021). Oleogel-based systems for the delivery of bioactive compounds in foods. *Gels, 7*(3), 1–24. https://doi.org/10.3390/gels7030086

Principato, L., Carullo, D., Bassani, A., Spigno, G., Gruppi, A., Duserm Garrido, G., & Dordoni, R. (2021). Effect of dietary fiber and thermal conditions on rice bran wax-based structured edible oils. *Foods, 10*(12). https://doi.org/10.3390/foods10123072

Ribeiro, D., Freitas, M., Silva, A. M. S., Carvalho, F., & Fernandes, E. (2018). Antioxidant and pro-oxidant activities of carotenoids and their oxidation products. *Food and Chemical Toxicology, 120*, 681–699. https://doi.org/10.1016/j.fct.2018.07.060

Rodriguez-Amaya, D. B. (2001). *A guide to carotenoid analysis in foods*. Washington: ILSI Press.

Rodriguez-Amaya, D. B., & Kimura, M. (2004). HarvestPlus handbook for carotenoid analysis. In *HarvestPlus technical monographs*. https://doi.org/10.1007/s00262-008-0513-6

Schjoerring-Thyssen, J., Zhang, W., Olsen, K., Koehler, K., Jouenne, E., & Andersen, M. L. (2020). Multiresponse kinetic modeling of heat-induced equilibrium of β-carotene cis-trans isomerization in medium-chain triglyceride oil. *Journal of Agricultural and Food Chemistry, 68*, 845–855. https://doi.org/10.1021/acs.jafc.9b05500

Shibasaki-Kitakawa, N., Kato, H., Takahashi, A., & Yonemoto, T. (2004). Oxidation kinetics of β-carotene in oleic acid solvent with addition of an antioxidant, α-tocopherol. *JAOCS, Journal of the American Oil Chemists' Society, 81*(4), 389–394. https://doi.org/10.1007/s11746-004-0911-x

Song, Z., Sarkar, S., Vogt, A. D., Danzer, G. D., Smith, C. J., Gualtieri, E. J., & Simpson, G. J. (2018). Kinetic modeling of accelerated stability testing enabled by second harmonic generation microscopy. *Analytical Chemistry, 90*(7), 4405–4413. https://doi.org/10.1021/acs.analchem.7b04260

Soto, C. C., Trasi, N. S., Schmitt, P. D., Su, Y., Liu, Z., Miller, E., Variankaval, N., Marsac, P. J., Simpson, G. J., & Taylor, L. S. (2017). Second harmonic generation microscopy as a tool for the early detection of crystallization in spray dried dispersions. *Journal of Pharmaceutical and Biomedical Analysis, 146*, 86–95. https://doi.org/10.1016/j.jpba.2017.07.066

Tavernier, I., Patel, A. R., Meeren, P. Van Der, & Dewettinck, K. (2017). Emulsion-templated liquid oil structuring with soy protein and soy protein : k -carrageenan complexes. *Food Hydrocolloids, 65*, 107–120. https://doi.org/10.1016/j.foodhyd.2016.11.008

Velasco, J., Andersen, M. L., & Skibsted, L. H. (2005). Electron spin resonance spin trapping for analysis of lipid oxidation in oils: Inhibiting effect of the spin trap α-phenyl-N-tert-butylnitrone on lipid oxidation. *Journal of Agricultural and Food Chemistry, 53*(5), 1328–1336. https://doi.org/10.1021/jf049051w

Vélez-Erazo, E. M., Bosqui, K., Rabelo, R. S., Kurozawa, L. E., & Hubinger, M. D. (2020). High internal phase emulsions (HIPE) using pea protein and different polysaccharides as stabilizers. *Food Hydrocolloids, 105*, Article 105775. https://doi.org/10.1016/j.foodhyd.2020.105775

Yi, J., Andersen, M. L., & Skibsted, L. H. (2011). Interactions between tocopherols, tocotrienols and carotenoids during autoxidation of mixed palm olein and fish oil. *Food Chemistry, 127*(4), 1792–1797. https://doi.org/10.1016/j.foodchem.2011.02.061

Zeb, A., & Murkovic, M. (2011). Carotenoids and triacylglycerols interactions during thermal oxidation of refined olive oil. *Food Chemistry, 127*(4), 1584–1593. https://doi.org/10.1016/j.foodchem.2011.02.022

Zeb, A., & Murkovic, M. (2013). Pro-oxidant effects of β-carotene during thermal oxidation of edible oils. *JAOCS, Journal of the American Oil Chemists' Society, 90*(6), 881–889. https://doi.org/10.1007/s11746-013-2221-4

Zetzl, A. K., Gravelle, A. J., Kurylowicz, M., Dutcher, J., Barbut, S., & Marangoni, A. G. (2014). Microstructure of ethylcellulose oleogels and its relationship to mechanical properties. *Food Structure, 2*(1–2), 27–40. https://doi.org/10.1016/j.foostr.2014.07.002

Zhang, K., Wang, W., Wang, X., Cheng, S., Zhou, J., Wu, Z., & Li, Y. (2019). Fabrication , physicochemical and antibacterial properties of ethyl cellulose-structured cinnamon oil oleogel : A relation of ethyl cellulose viscosity and oleogel performance. *Journal of the Science of Food and Agriculture, 99*(8), 4063–4071. https://doi.org/10.1002/jsfa.9636